

Experiments using a Finite Element Formulation of Incompressible Miscible Displacements in Porous Media

Adriana C. Barbosa, Lucia Catabriga, Andréa M. P. Valli

UFES - Departamento de Informática

Campus de Goiabeiras

29075-910, Espírito Santo, ES

E-mail: adriana@lcad.inf.ufes.br, luciac@inf.ufes.br, avalli@inf.ufes.br

Sandra Mara C. Malta

Depto de Mat. Aplicada e Comput., CMA, LNCC,

25651-075, Petrópolis, RJ

E-mail: smcm@lncc.br

Leonardo Muniz de Lima

Depto de Ciências Exata, UVV,

29102-770, Vila Velha, ES

E-mail: lmuniz@uvv.br

Summary: *This work presents a finite element implementation of incompressible miscible displacements in porous media. Through a predictor-multicorrector finite difference discretization in time, we use a sequentially implicit time-stepping algorithm that uncouples the system at each time-step. The Galerkin method is employed to approximate the pressure, and accurate velocity approximations are calculated using a post-processing technique taking into account a regularized initial solution for the concentration. A stabilized finite element (SUPG) method is applied to the convection-diffusion concentration equation. Numerical simulations of tracer injection processes and miscible displacements with high adverse mobility ratios in two dimensions are reported.*

Keywords: *Finite Element, Miscible Displacements, Post-Processing Technique*

1. Introduction

Reservoir simulation have been studied extensively for a number of authors in the last three decades. Miscible displacements which model enhanced oil recovery and tracer injection processes have been used for formulation, development and testing numerical since the early beginning of reservoir engineering. Different numerical methods were employed in miscible displacement simulations. Finite differences and control volume methods are the most used in commercial reservoir simulation, despite of their difficulties to solve complex geometries or the high costs to handle unstructured grids. Early finite element solutions for this problem are studied using different formulations. The concentration of the injected fluid in the mixture is the main variable. However, the calculation of Darcy's velocity, responsible for the transport, deserves special attention, since it has a strong influence on the stability and accuracy of the concentration approximation.

It has been proved through numerical analysis and computational simulations that the post-processing technique proposed in [4, 5, 6], computes accurate velocity fields when compared to those obtained by the usual methods found in the literature. Post-processing consists basically in solving the elliptic problem for pressure and then computing velocity considering residual forms of Darcy's law with the known pressure, the mass balance and irrotationality condition. Recently, many works revisited numerical methods for Darcy's flow. In particular, new stabilized mixed finite element formulations appear in many references, as in [1, 7]. However, differently from the mixed methods, which have a high computational cost due to the simultaneous solution of pressure and velocity, post-processing techniques are naturally segregated [5]. In this work we use the Galerkin method to approximate the pressure, and accurate velocity approximations are calculated using a post-processing technique taking into account a continuous initial

solution for the concentration. A stabilized finite element (SUPG) method is applied to the convection-diffusion concentration equation. Numerical simulations of tracer injection processes and miscible displacements with high adverse mobility ratios in two dimensions are reported.

2. Finite Element Approximations and Solution Algorithm

The mathematical model consists of an elliptic system coming from the conservation of mass, the Darcy's law and the conservation of the injected fluid. The governing equations for the miscible displacement of one incompressible fluid by another [8], in a porous medium $\Omega \in \mathbf{R}^2$ at an instant $t \in [0, T]$, can be described by

$$\nabla \cdot \mathbf{v} = q \quad \text{in } \Omega \times [0, T] \quad (1)$$

$$\mathbf{v} = -\mathbf{A}(c)\nabla p = -\frac{\mathbf{K}}{\mu(c)}\nabla p \quad \text{in } \Omega \times [0, T] \quad (2)$$

$$\phi \frac{\partial c}{\partial t} + \nabla \cdot (c\mathbf{v} - \mathbf{D}(\mathbf{v})\nabla c) = \hat{c}q \quad \text{in } \Omega \times [0, T] \quad (3)$$

with boundary and initial conditions

$$\mathbf{v} \cdot \mathbf{n} = 0 \quad \text{on } \partial\Omega \times [0, T] \quad (4)$$

$$\mathbf{D}\nabla c \cdot \mathbf{n} = 0 \quad \text{on } \partial\Omega \times [0, T] \quad (5)$$

$$c(\mathbf{x}, 0) = c_0(\mathbf{x}) \quad \text{in } \Omega \quad (6)$$

where $\mathbf{v} = (v_1, v_2)^T$ is the total Darcy velocity of the fluid mixture, p is the fluid pressure, c is the concentration of the fluid mixture, ϕ and \mathbf{K} are, respectively, the porosity and the permeability tensor of the porous medium, \mathbf{n} denotes the outward unit normal to $\partial\Omega$, q is the source and sink terms and \hat{c} is the injected concentration at injection wells and the resident concentration at production wells. The pressure equation is defined considering Eq. (2) into Eq. (1)

$$-\nabla \cdot (\mathbf{A}(c)\nabla p) = q \quad \text{in } \Omega \times [0, T] \quad (7)$$

Using the Leibniz rule, we can write $\nabla(c\mathbf{v}) = \mathbf{v} \cdot \nabla c + c\nabla \cdot \mathbf{v} = \mathbf{v} \cdot \nabla c + qc$. The non-divergence form of the concentration equation (3) considering the Leibniz rule can be rewritten as

$$\phi \frac{\partial c}{\partial t} + \mathbf{v} \cdot \nabla c - \nabla \cdot (\mathbf{D}(\mathbf{v})\nabla c) + \hat{c}c = \hat{c}q \quad \text{in } \Omega \times [0, T] \quad (8)$$

where $\hat{q} = \max(q, 0)$ is nonzero only at the injections wells. The diffusion-dispersion tensor \mathbf{D} is considered as in [8] for the 5-spot experiments

$$\mathbf{D} = \phi (\alpha_m \mathbf{I} + |\mathbf{v}| (\alpha_l \mathbf{E}(\mathbf{v}) + \alpha_t \mathbf{E}^I(\mathbf{v}))) \quad \mathbf{E}(\mathbf{v}) = \frac{1}{|\mathbf{v}|^2} \mathbf{v}\mathbf{v}^T \quad \mathbf{E}^I(\mathbf{v}) = \mathbf{I} - \mathbf{E}(\mathbf{v}) \quad (9)$$

where α_m , α_l , and α_t are, respectively, molecular diffusion, longitudinal, and transverse dispersion coefficients. Normally dispersion is physically more important than the molecular diffusion; also, α_l is usually considerably larger than α_t . In equation (2) $\mu = \mu(c)$ is the local viscosity of the mixture which depends on the concentration c of the injected fluid. In the reservoir simulation the empirical relation is usually adopted

$$\mu(c) = \mu(0) \left(1 - c + M^{1/4}c\right)^{-4}, \quad c \in [0, 1] \quad (10)$$

where $M = \mu(0)/\mu(1)$ is the mobility ratio. It is important to note that when $M > 1$ nonlinear effects associated to the coupling of equations and the convective term strongly influence stability and accuracy of numerical approximations. Since $p(x, t)$ is determined up to an arbitrary additive constant, we normalize it by imposing the condition $\int_{\Omega} p(x, t) dx = 0$, $t \in [0, T]$.

Introducing a standard finite element discretization for the domain Ω into subdomains Ω^e and a set of piecewise trial and weighting finite element spaces, the Galerkin formulation for the pressure equation (7) is

$$\int_{\Omega} \nabla w_p^h \cdot \mathbf{A}(c^h) \nabla p^h d\Omega = \int_{\Omega} w_p^h q d\Omega \quad (11)$$

where w_p^h is the discrete weighting function for pressure, and c^h and p^h are discrete counterparts of c and p . It is well known that computing the velocities directly from Darcy's law yields a low accuracy field, satisfying only weakly the no-flow boundary condition (see Eq. (4)). To improve the quality of the velocity approximation and still using standard Lagrangian bases we use here the global post-processing technique from [6], which can be summarized as follows. Given the Galerkin solution of the pressure p^h , the post-processed velocities \mathbf{v}^h are obtained from the variational statement as write in [2]

$$\int_{\Omega} \mathbf{w}_v^h (\mathbf{A}(c^h)^{-1} \mathbf{v}^h + \nabla p^h) d\Omega + \sum_{e=1}^{nel} \int_{\Omega^e} \nu_e \nabla \cdot \mathbf{w}_v^h (q - \nabla \cdot \mathbf{v}^h) d\Omega = 0 \quad (12)$$

where \mathbf{w}_v^h is the weighting function for post-processed velocities, ν_e a mesh dependent parameter of the magnitude $O(h)$ and nel is the number of elements in the mesh. The global post-processing technique numerical analysis presented by [6], indicates a gain of $O(h^{0.5})$ in the rates of convergence for velocity over mixed methods of Raviart-Thomas type.

The concentration equation (8) is predominantly advective and may exhibit sharp concentration fronts. Thus, we adopt the well known Streamline Upwind Petrov-Galerkin (SUPG) formulation enriched with the discontinuity operator CAU, that is given by

$$B(w_c^h, c^h) + \sum_{e=1}^{nel} \int_{\Omega^e} \tau \mathbf{v}^h \cdot \nabla w_c^h L(c^h) d\Omega + \sum_{e=1}^{nel} \int_{\Omega^e} \delta \nabla w_c^h \cdot \nabla c^h d\Omega = \int_{\Omega} w_c^h \hat{c} \hat{q} d\Omega \quad (13)$$

with

$$B(w_c^h, c^h) = \int_{\Omega} w_c^h L(c^h) d\Omega \quad \text{and} \quad L(c^h) = \phi \frac{\partial c^h}{\partial t} + \mathbf{v}^h \cdot \nabla c^h - \nabla \cdot (\mathbf{D}(\mathbf{v}^h) \nabla c^h) + \hat{q} c^h \quad (14)$$

where w_c^h is the weighting function for concentration and δ is the CAU discontinuity-capturing operator defined as in [3].

The spatial discretization of the pressure equation (11), the post-processing technique for velocities (12) and the concentration equation (13) lead to a set of coupled non-linear ordinary differential equation, as written in [2]:

$$\mathbf{K} \mathbf{p} = \mathbf{Q}, \quad \bar{\mathbf{M}} \mathbf{v} = \mathbf{F}_G + \mathbf{F}_q, \quad \tilde{\mathbf{M}} \dot{\mathbf{c}} + \tilde{\mathbf{C}} \mathbf{c} = \tilde{\mathbf{F}} \quad (15)$$

where \mathbf{p} , \mathbf{v} , \mathbf{c} and $\dot{\mathbf{c}}$ are the vector of unknown for the nodal values of the pressure, velocities, concentration and time derivative of the concentration, respectively. The matrix \mathbf{K} is symmetric, positive definite and depends on the concentration ($\mathbf{K} = \mathbf{K}(\mathbf{c})$). The right hand side vector \mathbf{Q} contains the flows rates and boundary conditions for the pressure equation. The post-processing matrix $\bar{\mathbf{M}}$ can be split in two matrices, $\bar{\mathbf{M}} = \mathbf{M}_w + \mathbf{M}_{div}$, where \mathbf{M}_w represents the contribution of the first integral of Eq. (12) and \mathbf{M}_{div} represents the part corresponding to the divergence weighting of the second integral of Eq. (12). The right hand side vectors \mathbf{F}_G and \mathbf{F}_q are respectively the weighting of the pressure gradients and the divergence weighting of the flow rates. The matrices $\tilde{\mathbf{M}}$ and $\tilde{\mathbf{C}}$ represent, respectively, time-dependent, convective and diffusive terms of the concentration equation. The matrix $\tilde{\mathbf{C}}$ depends on the velocity field ($\tilde{\mathbf{C}} = \tilde{\mathbf{C}}(\mathbf{v})$). The right hand side vector $\tilde{\mathbf{F}}$ is due to the boundary conditions. To solve the non-linear systems of ordinary differential equations (15) we employ a predictor-multicorrector finite difference discretization in time. For brevity, we present here only the block-iterative algorithm for the predictor-multicorrector method. To move from step n to $n + 1$, we need to solve the following steps:

Block 1: Solve the pressure equation

$$\mathbf{K}(\mathbf{c}_{n+1}^i) \mathbf{p}_{n+1}^{i+1} = \mathbf{Q}_{n+1} \quad (16)$$

Block 2: Compute the velocity field

$$\bar{\mathbf{M}}(\mathbf{c}_{n+1}^i) \mathbf{v}_{n+1}^{i+1} = \mathbf{F}_G(\mathbf{p}_{n+1}^{i+1}) + \mathbf{F}_q \quad (17)$$

Block 3: Solve the concentration equation

$$\mathbf{M}_{n+1}^* \Delta \hat{\mathbf{c}}_{n+1}^{i+1} = \tilde{\mathbf{F}}_{n+1} - \tilde{\mathbf{M}}(\hat{\mathbf{c}}_{n+1}^i) \hat{\mathbf{c}}_{n+1}^i - \tilde{\mathbf{C}}(\mathbf{v}_{n+1}^{i+1}, \mathbf{p}_{n+1}^{i+1}, \mathbf{c}_{n+1}^i) \mathbf{c}_{n+1}^i \quad (18)$$

where $\mathbf{M}_{n+1}^* = \tilde{\mathbf{M}} + \alpha \Delta t \tilde{\mathbf{C}}$ is the non-symmetric effective matrix.

Update:

$$\mathbf{c}_{n+1}^{i+1} = \mathbf{c}_{n+1}^i + \alpha \Delta t \Delta \hat{\mathbf{c}}_{n+1}^{i+1} \quad \text{and} \quad \hat{\mathbf{c}}_{n+1}^{i+1} = \hat{\mathbf{c}}_{n+1}^i + \Delta \hat{\mathbf{c}}_{n+1}^{i+1}. \quad (19)$$

In the expressions (16)-(19), i is the non-linear iteration count, Δt is the time step and α is a parameter that controls stability and accuracy of the time integration. We adopt here $\alpha = 0.5$, which is second-order accurate in time. The iterative process continues up to the i -th iteration where some convergence criteria are satisfied. The major computational tasks of the block-iterative algorithm are generation of the coefficient matrices and right hand side vectors. All matrices involved are built from element contributions. We consider linear triangles and one-point quadrature for integration. The element matrices computation can be carried out in closed form and all element matrices can be evaluated in a single loop.

3. Numerical Studies

To illustrate the efficiency of our numerical methodology, we solved a five-spot problem with two different mobility ratios: $M = 1$ and $M = 20$. The numerical experiments were performed in a quarter of a repeated five-spot pattern consisting of a square domain (unit thickness) with side $L = 1000.0 \text{ ft}$. The injector well is located at the lower-left corner ($x = y = 0$) and the producer well at the upper-right corner ($x = y = L$). In the experiments we use the Conjugate Gradient (CG) method to obtain the pressure solution in (16) and the Generalized Minimal Residual Method (GMRES) to solve the resulting non-symmetric systems for velocity field (17) and concentration (18). The tolerances for CG and GMRES(50) were taken as 10^{-6} and the tolerance for the predictor-multicorrector algorithm was set equal to 10^{-1} . All computations were performed on a Dell OptiPlex 740, with AMD Athlon 64 Dual-Core processor and a 1 MB *Cache*.

3.1 Tracer injection simulations ($M = 1$)

Firstly, in order to show the accuracy of our implementation we present simulation results for the tracer injection simulation [8]. To do this, a homogeneous porous medium with permeability $k = 100 \text{ mD}$, porosity $\phi = 0.1$, longitudinal dispersion $\alpha_l = 1.0 \text{ ft}$, transverse dispersion $\alpha_t = 0.0 \text{ ft}$ and molecular diffusion $\alpha_m = 0.0$ is considered. The viscosity of the resident fluid is $\mu(1) = 1.0 \text{ cP}$ and the mobility ratio is $M = 1$ (i.e. injected and resident fluids have the same properties). We consider a regular mesh with 80×80 squares, with each square divided into two linear triangles and time steps $\Delta t = 1.0 \text{ day}$. The flow rates are $f = 250 \text{ ft}^2/\text{day}$; thus, the tracer slug is 250 ft^3 corresponding 0.25% of the porous volume. Figure 1 shows the tracer configuration at $t = 800$ and $t = 1200$ days. As we have sharp concentration fronts, the prescribed boundary condition for the velocity field (see Eq. (4)) on the post-processing velocity block part (17) is crucial to determine an acceptable right solution, without spurious oscillations.

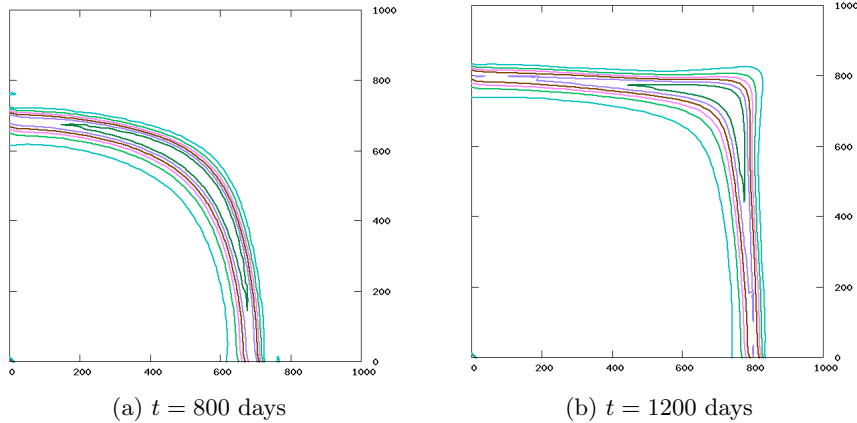


Figure 1: Concentration contours for the tracer injection problem.

3.2 Continuous injection simulations ($M > 1$)

In our second experiment we consider an adverse mobility problem with a continuous injection of the solvent at a flow rate of $200 \text{ ft}^2/\text{day}$. The same domain and properties of the previous example are considered, but the longitudinal and transverse dispersions are, respectively, $\alpha_l = 10.0 \text{ ft}$ and $\alpha_t = 1.0 \text{ ft}$. Thus, a pore volume of solvent is injected in 2000 days. The mobility ratio is $M = 20$ (the viscosity of the injected fluid is 20 times smaller than the viscosity of the resident one), the mesh is the same of the first experiment and $\Delta t = 1$ day. The situation now is totally different from the first case ($M = 1$), the problem is completely non-linear and, for example, some discontinuity of the initial condition can effect all the approximate solution, as we see in the study below. We will consider two different initial solutions ($c_0(\mathbf{x})$) for the concentration. Firstly, we set the concentration $c = 1$ at the injector well and $c = 0$ everywhere else, i.e., we employ a discontinuous initial function. Secondly, in order to remove this singularity on the injected well, we regularized the function considering a linear variation of the concentration for $c = 1$ to $c = 0$ on the radial direction close to the well.

We illustrate the efficiency of this proposal via the results presented in Figure 2, where iso-concentration curves at 500 and 1000 days are plotted. Figure 2 (**top**) shows the use of the discontinuous initial solution for the concentration and the post-processing technique for the velocity field. Thus, it is possible to see the very unstable concentration approximation due to the singularity on the injected well. A small improvement on the results are obtained when we combined the regularized initial solution with the Galerkin approximation for velocity field. However, some non-physical results still remain since the velocity approximation is very poor, as exhibited in Figure 2 (**middle**). Finally, Figure 2 (**bottom**) presents the most stable approximation for the concentration (physical acceptable) when the velocity field is given by the post-processing technique combined with the regularized initial solution.

To comment on the computational efficacy of our numerical approach, we show in Table 1 the average linear iteration numbers to solve pressure, CG, velocity field and concentration, GMRES(50), for the tracer injection problem ($M = 1$) along 1200 days and for the continuous injection problem ($M = 20$) along 1000 days. As we can see the number of linear iterations for pressure at $M = 20$ is much bigger than at $M = 1$. This follows directly from the strong non-linear character of the continuous injection problem.

4. Concluding Remarks

Numerical experiments for tracer injection ($M = 1$) and continuous injection with adverse mobility ($M > 1$) were performed to verify the accuracy of our finite element implementation of incompressible miscible displacements in porous media. We employ a second-order accu-

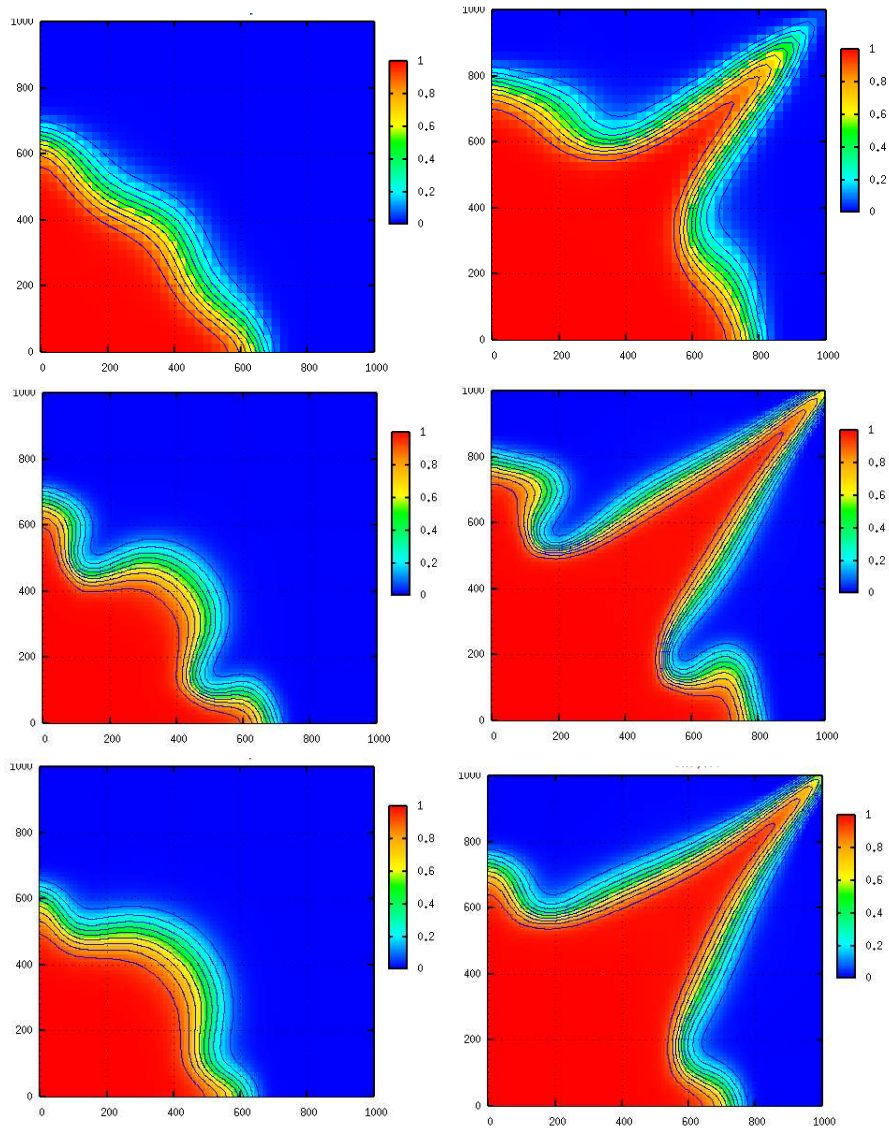


Figure 2: Iso-concentration curves at $t = 500$ days (left) and $t = 1000$ days (right): discontinuous initial solution combined with the post-processing technique (**top**); continuous initial solution combined with the Galerkin approximation for the velocity field (**middle**); and continuous initial solution combined with the post-processing technique (**bottom**).

Table 1: Average iteration numbers for tracer injection ($M = 1$) and continuous injection ($M = 20$) problems.

Mobility Ratio	Pressure	Velocity	Concentration	Time (Sec)
$M = 1$	189	72	30	1.934
$M = 20$	1594	85	15	4.246

rate in time predictor-multicorrector finite difference discretization to uncoupled the resulting non-linear finite element systems of ordinary differential equations. The Galerkin method is employed to approximate the pressure, and accurate velocity approximations are calculated using a post-processing technique taking into account a regularized initial solution for the concentration. A stabilized finite element (SUPG) method is applied to the convection-diffusion concentration equation. In the tracer injection problem was possible to observe the good agreement of the concentration contours. In the second problem, the numerical formulation was tested for a problem

with high nonlinearity with success. We showed in the experiments how some discontinuity of the initial concentration condition can effect all the approximate solutions even combined with the post-processing technique. However, stable approximation for the concentration (physical acceptable) can be obtained using a regularized initial solution and the velocity field given by the post-processing technique. We also verify that some non-physical results still remain when we combined the regularized initial solution with the Galerkin approximation for velocity field.

References

- [1] F. Brezzi, A. Masud, and T.J.R. Hughes. Mixed discontinuous galerkin methods for darcy flow. *Journal of Scientific Computing*, 22:119–145, 2005.
- [2] A.L.G.A. Coutinho and J.L.D. Alves. Finite element simulation of nonlinear viscous fingering in miscible displacements with anisotropic dispersion and nonmonotonic viscosity profiles. *Computational Mechanics*, 23:108–116, 1999.
- [3] A.C.R.N. Galeao and E.G. Do Carmo. A consistent approximate speed-up upwind petrov-galerkin method for convection-dominated. *Comp. Meth. Appl. Mech. Eng.*, 10:83–95, 1988.
- [4] A.F.D. Loula, A.L.G.A. Coutinho, and E.L.M. Garcia. Miscible displacement simulation by finite element methods in distributed memory machines. *Computer Methods in Applied Mechanics and Engineering*, 174:339–354, 1999.
- [5] S.M.C. Malta and A.F.D. Loula. Numerical analysis of the finite element methods for miscible displacement in porous media. *Numerical Method for Partial Differential Equations*, 14:519–548, 1998.
- [6] S.M.C. Malta, A.F.D. Loula, and E.L.M. Garcia. A post-processing technique to approximate the velocity field in miscible displacement simulations. *Contemporary Mathematics*, 8:239–268, 1995.
- [7] A. Masud and T.J.R. Hughes. A stabilized mixed finite element method for darcy flow. *Computer Methods in Applied Mechanics and Engineering*, 191:4341–4370, 2002.
- [8] D.W. Peaceman. *Survey of problems in numerical reservoir simulation*. SIAM, Philadelphia, 1986.